NRL Memorandum Report 6491

Energy Transfer from High Power Pulselines to the Next Generation of PRS Loads

R.E. TERRY

Plasma Radiation Branch
Plasma Physics Division

F.L. COCHRAN

Berkeley Research Associates

June 15, 1989

This research was sponsored by the Defense Nuclear Agency, under Subtask Code and Title: RL RB/Advanced Technology Development, Work Unit Code 00079, MIPR No. 89-565.

Approved for public release; distribution unlimited.

SECURITY CLASSIFICATION OF THIS PAGE

REPORT DOCUMENTATION PAGE

Form Approved OMB No. 0704-0188

1a REPORT SECURITY CLASSIFICATION UNCLASSIFIED	1b RESTRICTIVE MARKINGS
2a. SECURITY CLASSIFICATION AUTHORITY	3 DISTRIBUTION/AVAILABILITY OF REPORT Approved for public release; distribution unlimited.
2b. DECLASSIFICATION/DOWNGRADING SCHEDULE	
4. PERFORMING ORGANIZATION REPORT NUMBER(S) NRL Memorandum Report 6491	5. MONITORING ORGANIZATION REPORT NUMBER(S)
6a. NAME OF PERFORMING ORGANIZATION Naval Research Laboratory 6b. OFFICE SYMBOL (If applicable) Code 4720	7a. NAME OF MONITORING ORGANIZATION
6c. ADDRESS (City, State, and ZIP Code) Washington, DC 20375-5000	7b ADDRESS (City, State, and ZIP Code)
8a. NAME OF FUNDING/SPONSORING ORGANIZATION Defense Nuclear Agency 8b OFFICE SYMBOL (If applicable) RAEV	9 PROCUREMENT INSTRUMENT IDENTIFICATION NUMBER
8c. ADDRESS (City, State, and ZIP Code)	10 SOURCE OF FUNDING NUMBERS PROGRAM ELEMENT NO: 62715H PROJECT NO: TASK NO: WORK UNIT ACCESSION NO: DN880-191

11. TITLE (Include Security Classification)
Energy Transfer from High Power Pulselines to the Next Generation of PRS Loads

12 PERSONAL AUTHOR(S)
Terry, R.E. and Cochran,* F.L.

13a TYPE OF REPORT	13b TIME COVERED	14 DATE OF REPORT (Year, Month, Day)	15 PAGE COUNT
Interim	FROM ____ TO ____	1989 June 15	29

16 SUPPLEMENTARY NOTATION
(See page ii)

17 COSATI CODES			18 SUBJECT TERMS (Continue on reverse if necessary and identify by block number)
FIELD	GROUP	SUB-GROUP	Plasma radiation source; Inductive energy storage; Saturn pulseline; Power flow

19 ABSTRACT (Continue on reverse if necessary and identify by block number)

The efficiency of energy transfer to model PRS loads on high power pulselines is investigated with a series of PRS models and a transmission line code.

20 DISTRIBUTION/AVAILABILITY OF ABSTRACT ☒ UNCLASSIFIED/UNLIMITED ☐ SAME AS RPT ☐ DTIC USERS	21 ABSTRACT SECURITY CLASSIFICATION UNCLASSIFIED	
22a NAME OF RESPONSIBLE INDIVIDUAL Dr. Jack Davis	22b TELEPHONE (Include Area Code) (202) 7673278	22c OFFICE SYMBOL Code 4720

DD Form 1473, JUN 86 — Previous editions are obsolete — SECURITY CLASSIFICATION OF THIS PAGE

S/N 0102-LF-014-6603

SECURITY CLASSIFICATION OF THIS PAGE

16. SUPPLEMENTARY NOTATION

*Berkeley Research Associates

This research was sponsored by the Defense Nuclear Agency, under Subtask Code and Title: RL RB/Advanced Technology Development, Work Unit Code 00079. MIPR No. 89-565.

CONTENTS

ENERGY TRANSFER FROM HIGH POWER PULSELINES TO THE NEXT GENERATION OF PRS LOADS

I. Introduction

The design of more complex loads for Plasma Radiation Sources and the quest for ever higher simulator radiative yields and power levels require heretofore unexplored energy densities in the load region, perhaps as high as 1.50 MJ/cm^3. Quite apart from detailed design questions, there is some concern that these higher power and energy densities (delivered by "sub-Ohm" pulselines) cannot couple well to the PRS configurations used today[1] or to even higher inductance designs that might be used in the future.

In this report we will examine the energy transfer to two PRS loads from generic pulselines of the Saturn class operating at the 8 → 15 MA level. Saturn is nearly a 10x machine in terms of power flows and has recently been outfitted with PRS front end hardware; it is modeled in a subsequent section (III). A basic slug PRS model and an appropriate X-pinch model, derived from 2-D MHD simulations, are used.

The pulselines are modeled with a transmission line code, described in the next section (II). Apart from generalization to spacetime dependent line parameters (impedance, propagation speed, and damping), the solution technique is quite standard, robust, and accurate in its energy transfer characteristics. Even the simplest transmission line models of machines like Saturn provide the expected result - PRS loads will accommodate the line impedance and draw energy effectively. A more delicate question is that of loss mechanisms. This is left to future work.

In Section IV the coupling of pulsers like Saturn or the Falcon design (proposed by PI as a 10x device) to an X-pinch load is discussed. The particular load chosen is first modeled with the 2-D MHD code PRISM to exhibit the behavior we wish to exploit. The inductance history can then be used as a rough guide to the behavior

Manuscript approved November 29, 1988.

of such loads in Saturn or Falcon class machines.

Section V is devoted to a discussion of the results, conclusions and the implications for future efforts.

II. Transmission Line Model

Existing transmission line models come in several variations. Within the MAGIC [2] program exist options for coupling transmission lines to a variety of 2-D simulation regions as well as the use of parallel and series junctions among lines. Within the BERTHA [3] package exists a broad spectrum of line elements on which waves are propagated without distortion by summation of forward and backward disturbances. In any study of energy coupling to the time dependent PRS one must join the transmission line to varying load parameters Z(t), L(R(t)), allow for space time varying line parameters, and also drive the system with a fixed initial energy. No existing transmission line code offered ready access to all these capabilities, so a simple implementation of the 1-D telegrapher's equations has been written to treat such problems.

Resolving the continuous transmission line into discrete units of inductance per unit length (L') in series with the load and capacitance per unit length (C') in parallel with the load, the telegrapher's equations can be written in the dimensionless forms

$$ {}^{n+1}V_j = {}^{n}V_j - \alpha Z_j \left({}^{n+1/2}I_j - {}^{n+1/2}I_{j-1} \right) , $$

$$ (\mathcal{D}_- \, {}^{n+1/2}I)_j = (\mathcal{D}_+ \, {}^{n-1/2}I)_j - \frac{\alpha}{Z_j} \left({}^{n}V_{j+1} - {}^{n}V_j \right) , $$

where the matrix operator

$$ \mathcal{D}_\pm = (\mathcal{I} \pm \gamma\alpha \, \nabla^2)_{ij} \quad , $$

introduces an adjustable damping parameter

$$\gamma \approx \frac{1}{8} \propto \frac{k_{Nyq}}{k_{damp}}$$

which controls the dispersion of the method at high wavenumber. By damping out the large wave number components, the tendency of these difference equations to propagate higher wavenumbers more slowly is mitigated and low wavenumber pulse shapes are then transmitted with low harmonic distortion. Here the parameter $\alpha = ch_t/h_x$ *is the Courant number, and* Z_j *can be spatially and temporally variable.*

At the boundaries the damping is set to zero, the combination of exterior circuit elements and the local currents on the transmission line then fixes the time advanced currents and voltages through:

$$^{n+1/2}I_o = {}^{n-1/2}I_o - \frac{\alpha}{Z_o}\left({}^nV_1 - {}^nV_o\right) ,$$

$$^{n+1/2}I_J = {}^{n-1/2}I_J - \frac{\alpha}{Z_J}\left({}^nV_{J+1} - {}^nV_J\right) ,$$

$$^nV_o = \frac{Z_o\tau V_s(t) + L_o^n V_1}{Z_o\tau + L_o} ,$$

$$^nV_{J+1} = \frac{\tau Z_J\, {}^nI_J Z_L(t) + L(R)^n V_J}{\tau Z_J + L(R)} ,$$

where the time derivative of current has been eliminated in favor of the appropriate voltage differences and τ *is the delay interval of a single element, viz.* $\tau = h_x/c$. *The source voltage* $V_s(t)$ *can be derived through a variety of methods, e.g., a fixed waveform, or a computed capacitive discharge. The load is characterized by a time dependent inductance* $L(R,t)$ *and resistance* $Z_L(t)$. *Here* R *denotes the load radius, and* $\dot{R}$ *must be included in the load resistance.*

For a PRS load a wide variety[4-8] *of simple models has been used in this context. Each choice made in configuring the load model has consequences for the calcu-*

lation as a whole which are substantially impossible to generalize and which produce a variety of transmission line responses. In order to set the proper damping parameter and thus to calibrate the basic method, a simpler problem is appropriate.

If the input voltage is specified as a Gaussian pulse with a variable width relative to the transmission line time and the load is a fixed impedance equal to that of the transmission line, then the ideal response is a distortion free propagation of the Gaussian pulse. Given an upper limit to the wavenumber which can be resolved by the difference equations, the damping added must attenuate the higher wavenumber components enough to prevent the "shedding" of aphysically slow "wake" disturbances, but not so large as to interfere with an accurate portrayal of the energy transport in the line.

The use of a γ value of about 0.125, corresponding to a damping wavenumber at about 4 times the Nyquist wavenumber, offers a reasonable compromise in this tradeoff. With an overall energy conservation error of $5.15 \cdot 10^{-4}$, Figure 1 shows the result of propagating a 50 ns pulse over a 22.5 ns length of $1/8\ \Omega$ line into a matched load. The Gaussian envelope at the output is essentially self-similar to that at the input, being scaled down slightly due to the attenuation in the method. There are no reflections at the interface for the matchload at any part of the wavenumber spectrum.

Figure 1

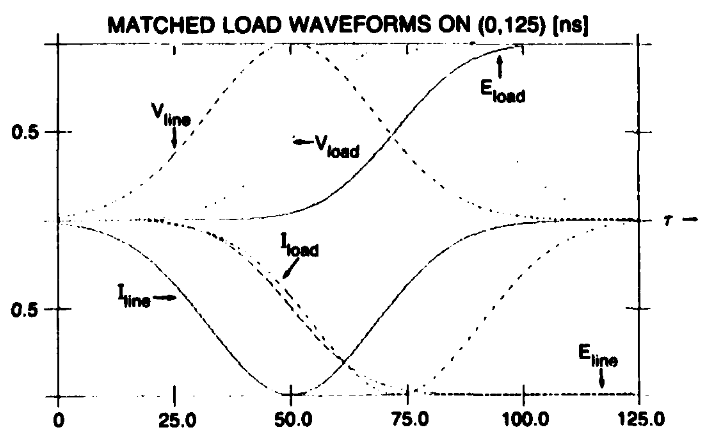

III. Application to Saturn

A simple model of the Saturn machine at SNL can be formed from three elements: a pulse source, a long transmission line section equivalent to the four parallel water lines which bring the power down to a radius of 1 m, and a short transmission line delivering the power to the load region which, in the PRS mode, offers an initial inductance of 5→10 nH.

In practice the transition between the two lines is a post-hole convolute, while the shorter line offers a fixed impedance for only part of the path to the load, after which it becomes a simple radial line, viz. $Z \propto 1/R$. *The details of the Marx bank will be ignored here – let it be abstracted to a single fast pulse (4.4 MV and 50 ns* $\frac{1}{e}$ *width) in series with a small resistance (0.12 Ω). Likewise, the convolute details will be ignored as well, it is abstracted to a discrete jump in impedance to 3.3 Ω, up from the 1/4 Ω of the parallel water lines.*

In terms of detailed experimental support such minutiae as these are important, but in this examination of gross power coupling they will not matter and they are modeled [9] elsewhere. The primary quest here is the energy coupling characteristics of Saturn class machines to various PRS configurations. The simplest adequate model can therefore be abstracted to the following transmission line problem.

Figure 2

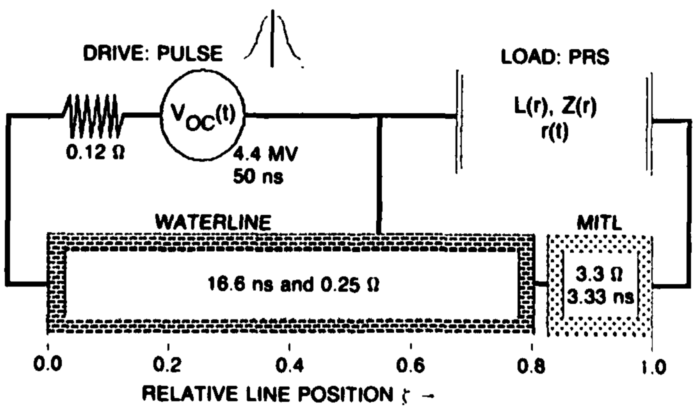

To drive 10x machine currents to a PRS load in $\approx 100ns$ requires $V_{oc} \approx 4MV$ on the driver pulse, and a forward energy fluence of $\approx 1MJ$ into the waterline.

As a further benchmark test of the transmission line code, a similar problem was run on the BERTHA package[10] with an 1/8 Ω line impedance and a fixed load impedance of 3/8 Ω. Both calculations agree to a few percent in the timing of various reflections, the timing of current reversals and in the peak values of the voltage and current waveforms (at the input to the line and at the load).

Slug PRS Model

The early phase of implosion presumes a snowplow like compression of the full load mass. Even though such an idealization is not likely to be completely accurate, for several reasons, the most serious consequence is a shift of the optimum mass point for radiation yield. The most important variable in the calculation of the run down is the motional impedance. I have shown elsewhere[11] that a variety of details in the current penetration and radiation physics still allows a rough adherence to the familiar snowplow velocity scaling with electric field – either for a slug or for a fully resolved 1-D load model. As a consequence the slug model will capture the proper trends in generator/load coupling even if the point by point comparisons may differ somewhat from the actual experiment.

Employing a series resistance and inductance for the slug load, both time varying as determined by the load radius, the governing equations for the run down phase become:

$$\ddot{R} = -\frac{I^2}{\mu c^2 R} ,$$

$$L(R) = \frac{2d}{c^2} \ln(\frac{R_{wall}}{R}) ,$$

$$Z_L = Z_o - \frac{2d}{c^2}\frac{\dot{R}}{R} ,$$

with Z_o fixed, d the AK gap, R_{wall} the radius of the return current path in the load region, μ the load mass per unit length, and Z_o the average impedance of the plasma, viz. $Z_o = \frac{\eta d}{\pi R^2}$. The choice η is reasonably taken to produce a Z_o in the 10mΩ range at early times. Coupling the relations to the transmission line solver is accomplished by calculating R, $\dot{R}$, Z_L and $L(R)$ at each timestep. The energy absorbed in the load region is then $\int^t dt_1\ V_L(t_1)I_L(t_1)dt_1$ as inferred from the line solution.

As the run-down terminates the plasma load should ideally undergo a non-adiabatic stagnation and convert the input energy to radiation. The final state of the load plasma is almost never very simple, but a rough average picture is to model it as a Bennet equilibrium pinch. The Bennet current figures as a central notion in oscillatory MHD solutions as well, so an order of magnitude sort of model can set the final impedance at a fixed final radius, R_{min}. If the pinch temperature is eliminated in favor of the current, one finds that the Bennet profile offers an impedance

$$Z_L = 1.109 \cdot 10^9 \left(\frac{d\ \mu^{3/2}}{R_{min}^2 I_{kA}^3} \right) [\Omega] \ ,$$

where I_{kA} is in units of kA, R_{min} is chosen initially, and the motional impedance is assumed to vanish.

Energy Coupling and Stagnation Radius

The radial structure of a PRS load will generally have a substantial effect on the radius of the current path at stagnation. Efficient radiative loss can deepen the implosion by perhaps a factor of 10; turbulent enhancement of plasma resistivity can spread the current channel and increase the final radius. While the final radius is therefore not a "free" parameter is any sense, it is a very relevant measure of the *implosion quality. Moreover, the logarithmic singularity in the load inductance as $R_{min} \to 0$ makes this parameter appear to be important for energy transfer. While the values of R_{min} examined here are a bit smaller than those observed in practice, the machine behavior expected if very small radii are achieved is a worthwhile target in a study of this kind.*

On the transmission line, the load implosion and stagnation appears as a backward propagating pulse – lowering the current and increasing the voltage. As the load samples larger inductance values due to smaller R_{min} this "downward" current pulse turns into a full current reversal. The larger R_{min} values thus imply a mild power reflection back up the line, while the smaller values imply a rather effective rejection of power by the load.

Figure 3(a,b) .... Figure 4(a,b)

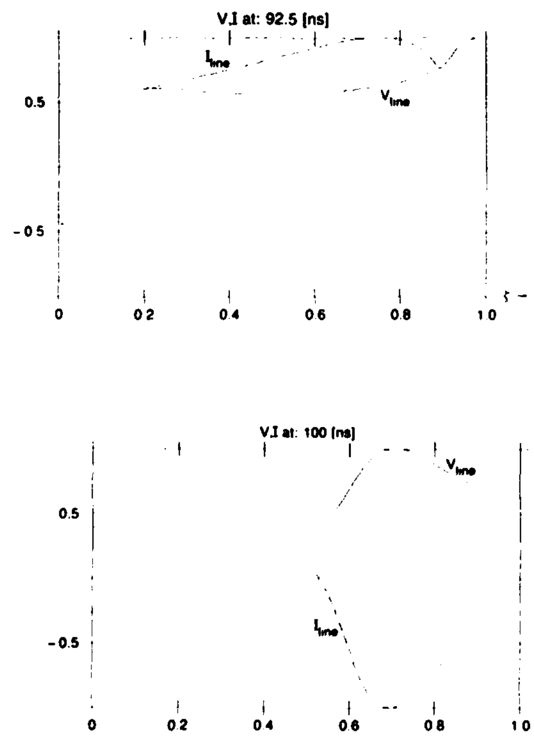

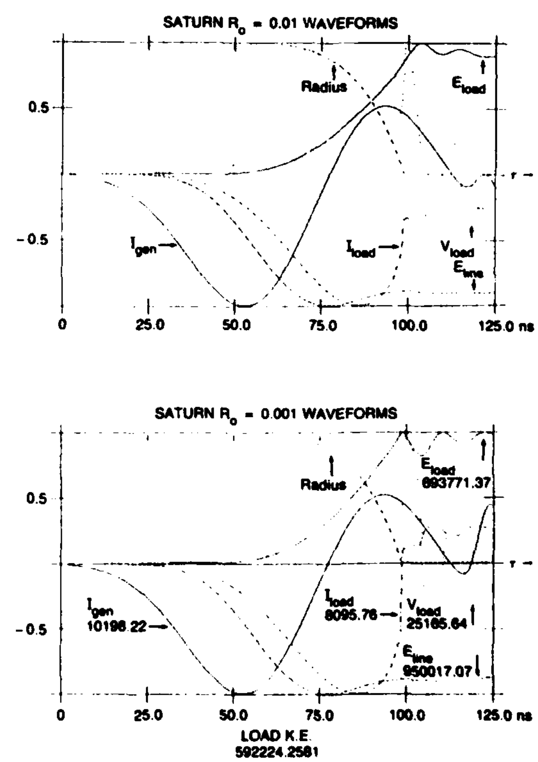

In Figure 3 are two snapshots of the reflection in a Saturn calculation, one at $R_{min} = 0.01cm$*, the other at* $R_{min} = 0.001cm$*. In Figure 4 are shown the drive and load I and V waveforms, as well as the energy into the line and into the load. The load radius is also plotted. All such runs as these were done with a load mass of 100* $\mu g/cm$ *and produced a peak load current* $\approx 8MA$*. The mass is such that implosion occurs at* $\approx 100ns$ *and the reflected power is therefore unable to go up and back before the run ends at 125 ns.*

Under the assumptions of this PRS model, when the load reverses the current the energy leaves the load region because all the energy is in the fields around it. The real behavior would likely be more dissipative and not allow as much energy release to the line. It is therefore reasonable to compare the energy coupled to the load region to that coupled to a $1/4\ \Omega$ *matched load in the constant 125 ns interval. The results are summarized in the following Figure 5, where the efficiencies of overall energy transfer -* $\eta_L = E_{Load}/E_{match}$ *- and transfer to load kinetic energy -* $\eta_T = T_{PRS}/E_{match}$ *are plotted.*

Figure 5

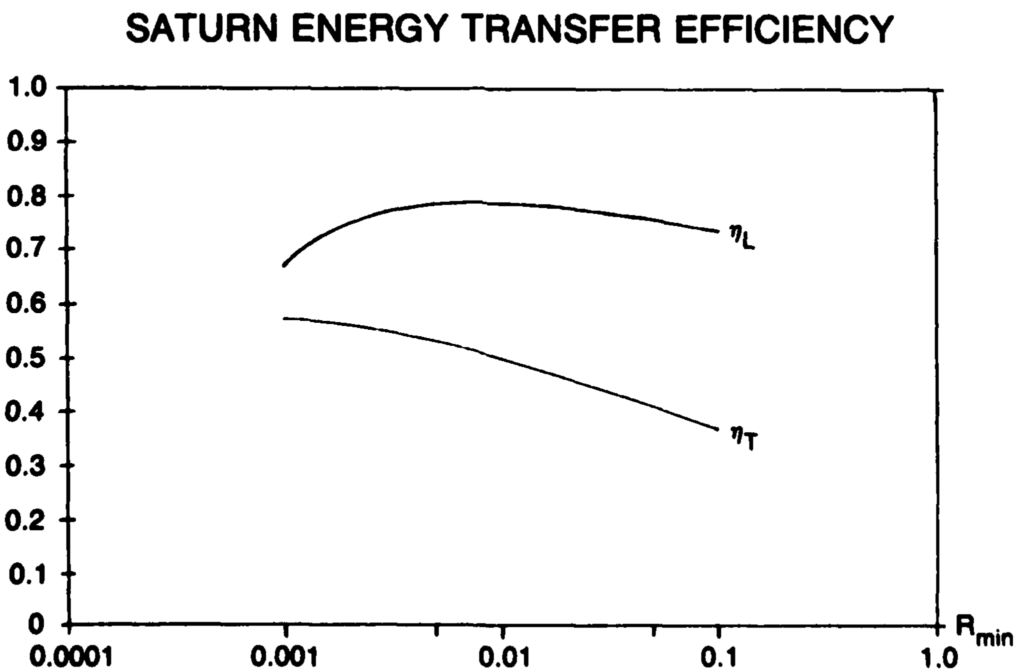

IV. X-pinches in Saturn and Falcon

The X-pinch load has heretofore been configured[12,13] *as two or more crossed wires in a diode gap. The central motivation being to focus more of the machine power on a smaller volume of plasma in hopes of exciting more K-shell radiation. A different quest for the X-pinch can also be contrived – the production of a "mini-diode" plasma state which will make effective use of nonthermal electron populations in exciting K-shell radiation.*

In order to produce such a "mini-diode" one can exploit the sausage instability through judicious mass loading. Using the simple scaling law for the implosion time pointed out by Apruzese[7]*, a constraint of fixed time from different radii imposes a particular mass per unit length on any extended load configuration –*

$$\mu_o = 1.1972 \cdot 10^3 \left(\frac{\tau_o I_p}{R_o}\right)^2 \ [\mu g/cm] \ ,$$

such that, for a fixed run down time τ_o to a peak current I_p, a figure of revolution $R_o(Z)$ must be mass loaded as above in order to implode synchronously at all axial locations. In Figure 6 are shown the density contours of such a load exactly as it was represented in the 2-D MHD code PRISM. The conical portion helps to keep the inductance lower at early times, while the cylindrical segment near the midplane is allowed a greater or lesser rundown length to provide a store of kinetic energy upon stagnation.

Figure 6

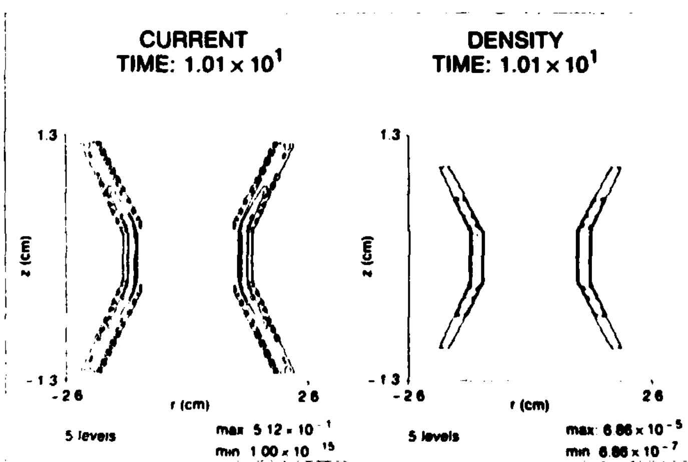

This load configuration was imploded through the use of a current ramp which rose linearly to 3 MA in 100 ns. While there is certainly some detailed structure produced during the rundown, the dominant kinematics is precisely as inferred from the 0-D scaling law. By 90 ns (c.f. Figure 7), the conical portion has run down a bit faster and two density peaks have appeared about the midplane. Some material

Figure 7,8,9

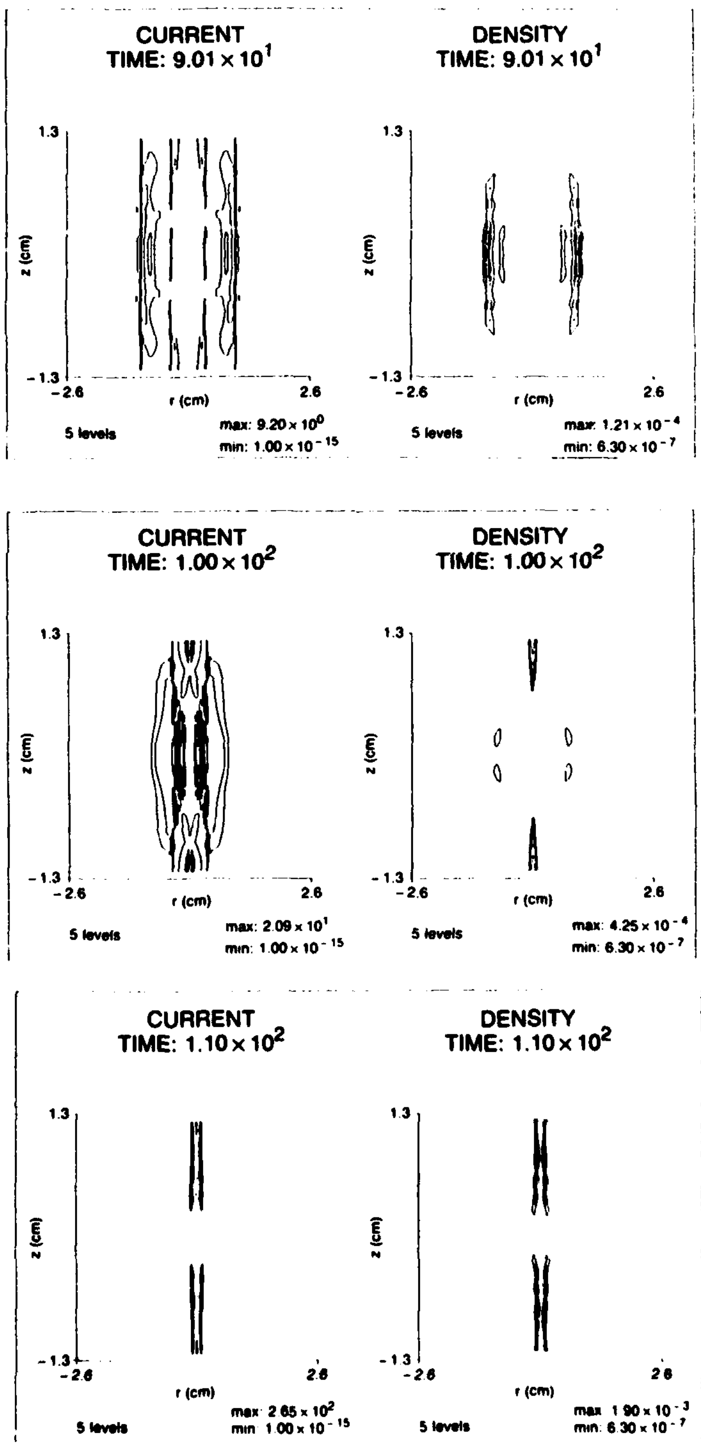

has been pushed ahead near the midplane due to magnetic field penetration and the resulting spallation when the shock emerged into the interior.

Upon stagnation at about 100 ns the load dynamics does reflect the structural details impressed during the rundown. The sausage instability goes rapidly to a saturated state – the current density is shown to leave the necked down region – and the originally cylindrical segment is bifurcated, c.f. Figure 8. The split state persists for some 10 ns more through the end of the simulation, Figure 9.

Here "stagnation" connotes the arrival of material on axis, the history of the density there is shown in Figure 10. The overall load design has thus produced its intended result – there is a density cavity of nearly two orders of magnitude near the midplane over which the diode voltage must be dropped!

Figure 10

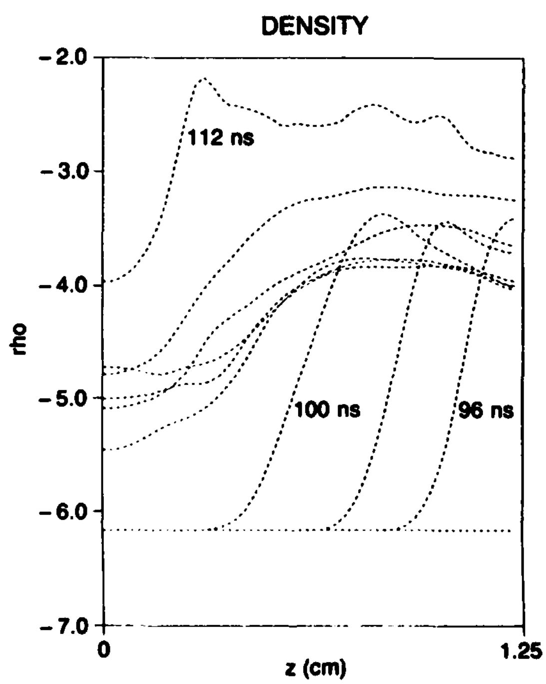

We leave to future work the assessment of runaway electron populations in such a load. For now, in the context of a 10x machine, it is reasonable to examine the energy delivery to such a load when it is characterized by a time dependent inductance and the implied motional impedance. When the evolution in 2-D shown above is reduced to an inductance history one finds the behavior shown in Figure 11. There is shown the inductance added by the imploding X-pinch and a similar (in mass, radius and current) slug implosion.

For the model to work with the transmission line code this function must be mapped into the familiar triad [$L(R)$, $Z_L(R,\dot{R})$, and $R(t)$]. The radius we use is a current weighted one, viz. derived from the volume exterior to the current channel.

Figure 11

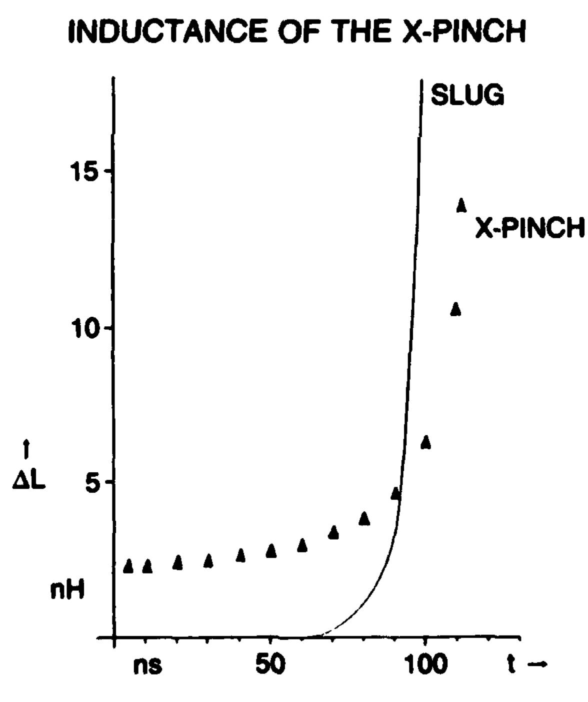

Saturn X-pinch

When the X-pinch model is used in place of the slug in the same machine simulation of Saturn detailed above, the energy transfer is somewhat lower due to the lack of enough motional impedance to draw energy from the line. The overall waveforms are shown in Figure 12, and the inductive "notch" is much less pronounced. The inferred efficiency η_L is 0.45, and the peak load current is $8.3MA$.

Figure 12

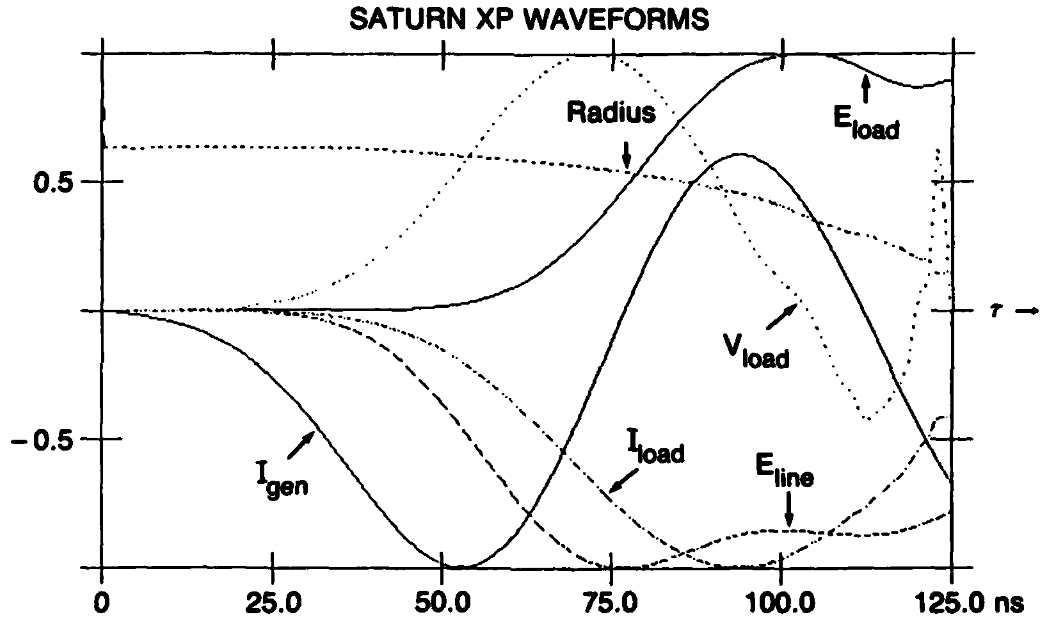

Falcon X-pinch

Since the Falcon design is concerned with an inductive storage device, the circuit and transmission line model changes slightly. In a Falcon 10x machine eight inductive energy stores (IES) are switched together into a single MITL at about a meter radius which then must converge the power to a PRS load. The IES modules would have a quarter period of $\approx 1.27\mu s$, *each being charged to perhaps 720 kV and using a storage inductor of about 150 nH in vacuum prior to the opening switch. A reasonably generous estimate of the inductance downstream of the opening switch (before the PRS load implodes) is perhaps 18 nH. Thus, working from a meter radius or 3 ns, the final transmission line impedance is 6* Ω.

When all eight modules are connected and switched out near peak current one has some 30 MA available to drive the final line and PRS. Not all of this current is expected in the imploding load, most of the energy will be dissipated in the opening switch or left in the inductance of the store and final transmission line. However, even with all these sinks the final energy to an imploding load is easily competitive with Saturn. If, for example, the Falcon opening switch were to achieve an $\dot{R} \approx 0.05\Omega/ns$, *the energy delivery efficiency to a slug load* (η_L), *relative to the original stored energy, is* ≈ 0.46 *– in the same range that Saturn achieves into a slug load. This efficiency is computed over the same time interval,* $[0, 125]ns$, *and decays with slower opening rates. If the X-pinch load is examined at the same opening rate, the efficiency decays to* ≈ 0.36. *The peak current expected in the Falcon X-pinch would be* $\approx 17.0MA$, *again comparable to Saturn.*

V. Conclusions

All the experience to date with this transmission line and load model indicates that for all of the generic machine designs presently contemplated for the 10x ma-

chine, for all the likely domains of load stagnation radius, one can state two results with some confidence.

- *The front end inductance of a PRS load per se is not a problem for energy coupling, provided this inductance remains in the range $\leq$20nH.*
- *The gas puff PRS load on Saturn should draw at least 8$\rightarrow$10 MA in the present configuration.*

The observed behavior[14] on Saturn – 10 MA into gas puffs and 12.5 MA into short circuit loads – is quite nicely in line with this prediction.

Furthermore, all the experience to date with the more complex X-pinch load design indicates that (i.) it represents a very credible PRS concept in terms of energy coupling and (ii.) it should be quite compatible with the presently contemplated 10x machine designs. The model we have discussed here will be refined further by 2D MHD studies to include the role of runaway electron populations in the energy budget and to optimize the load dynamics.

More general problems, involving loss mechanisms in MITL segments, can be readily addressed by the method and some initial work is already underway.

References

1. *Theoretical and Experimental Comparison of GAMBLE II Argon Gas Puff Experiments, J. W. Thornhill, et. al., NVOO Proceedings, to be published, 1988.*
2. *MAGIC Users Manual, B. Goplen, et. al., MRC/WDC-R-126.*
3. *D. D. Hinshelwood, NRL Memo Rep. 5185, 1983, "BERTHA – A Versatile Transmission Line and Circuit Code".*
4. *D. Mosher, NRL Memo Rep. 3687, 1978, "Coupling of Imploding-Plasma Loads to High-Power Generators".*
5. *R. E. Terry and J. U. Guillory, "Development and Exploration of the Core-Corona Model of Imploding Plasma Loads," DNA Report 5234F, 1980.*
6. *J. U. Guillory and R. E. Terry, "Modeling of Imploded Annular Plasmas," DNA Report 6152F, 1982.*
7. *J. P. Apruzese and J. Davis, NRL Memo Rep. 5406, 1984, "K-Shell Yield Scaling Law for Conventional PRS Loads".*
8. *S. W. McDonald and P. F. Ottinger, NRL Memo Rep. 5785, 1986, "Modeling and Simulation of an Imploding Plasma Radiation Source".*
9. *P.Corcoran,et. al., Pulse Sciences Rep. PSI-FR390-05, Oct 1988, "Sandia Double Post Hole Convolute Puff Diode, Final Electrical and Mechanical Design"*
10. *A. E. Robson, private communication.*
11. *R. E. Terry, et. al., Bull. APS, 1984, "Velocity Scaling of the Radiatively Dominated Z-Pinch".*
12. *K. G. Whitney, J. Davis, and N. R. Pereira, NRL Memo Rep. 5970, 1987, "New Load Design Concepts for Z-Pinches."*

13. N. Loter, et. al. and J. Davis, et. al., *Maxwell Laboratory Rep. MLR-3017, "Advanced Wire Experiments on Blackjack 5", 1988.*

14. P. Spence, R. Spielman, private communication.

DISTRIBUTION LIST

Assistant to the Secretary of Defense Atomic Energy Washington, D.C. 20301 Attn: Executive Assistant	1 copy
Director Defense Nuclear Agency Washington, D.C. 20305	
Attn: DDST	1 copy
TITL	4 copies
RAEV	1 copy
STVI	1 copy
Commander Field Command Defense Nuclear Agency Kirtland AFB, New Mexico 87115 Attn: FCPR	1 copy
Chief Field Command, Livermore Division Department of Defense Post Office Box 808 Livermore, California 94550 Attn: FCPRL	1 copy
Director Joint Strat TGT Planning Staff Offutt AFB Omaha, Nebraska 68113 Attn: JLKS	1 copy
Undersecretary of Defense for RSCH and ENGRG Department of Defense Washington, D.C. 20301 Attn: Strategic and Space Systems (OS)	1 copy
Deputy Chief of Staff for RSCH DEV and ACQ Department of the Army Washington, D.C. 20301 Attn: DAMA-CSS-N	1 copy
Commander Harry Diamond Laboratories Department of the Army 2800 Powder Mill Road Adelphi, Maryland 20783 Attn: DELHD-N-NP DELHD-R J. Rosado DELHD-TA-L (Tech. Lib.)	1 copy each

U.S. Army Missile Command Redstone Scientific Information Center Attn: DRSMI-RPRD(Documents) Redstone Arsenal, Alabama 35809	3 copies
Commander U.S. Army Nuclear and Chemical Agency 7500 Backlick Road Building 2073 Springfield, Virginia 22150 Attn: Library	1 copy
Commander Naval Intelligence Support Center 4301 Suitland Road, Bldg. 5 Washington, D.C. 20390 Attn: NISC-45	1 copy
Commander Naval Weapons Center China Lake, California 93555 Attn: Code 233 (Tech. Lib.)	1 copy
Officer in Charge White Oak Laboratory Naval Surface Weapons Center Silver Spring, Maryland 20910 Attn: Code R40 Code F31	1 copy each
Air Force Weapons Laboratory Kirtland AFB, New Mexico 87117 Attn: SUL CA APL Lt. Col Generosa	1 copy each
Deputy Chief of Staff Research, Development and Accounting Department of the Air Force Washington, D.C. 20330 Attn: AFRDQSM	1 copy
Commander U.S. Army Test and Evaluation Command Aberdeen Proving Ground, Maryland 21005 Attn: DRSTE-EL	1 copy

AVCO Research and Systems Group 201 Lowell Street Wilminton, Massachusetts 01887 Attn: Library A830	1 copy
BDM Corporation 7915 Jones Branch Drive McLean, Virginia 22101 Attn: Corporate Library	1 copy
Berkeley Research Associates Post Office Box 983 Berkeley, California 94701 Attn: Dr. Joseph Workman	1 copy
Berkeley Research Associates Post Office Box 852 5532 Hempstead Way Springfield, Virginia 22151 Attn: Dr. Joseph Orens	1 copy each
Boeing Company Post Office Box 3707 Seattle, Washington 98134 Attn: Aerospace Library	1 Copy
The Dikewood Corporation 1613 University Blvd., N.E. Albuquerque, New Mexico 87110 Attn: L. Wayne Davis	1 copy
General Electric Company - Tempo Center for Advanced Studies 816 State Street Post Office Drawer QQ Santa Barbara, California 93102 Attn: DASIAC	1 Copy
Institute for Defense Analyses 1801 N. Beauregard Street Alexandria, Virginia 22311 Attn: Classified Library	1 copy
IRT Corporation Post Office Box 81087 San Diego, California 92138 Attn: R. Mertz	1 copy
JAYCOR 1608 Spring Hill Road Vienna, Virginia 22180 Attn: R. Sullivan	1 copy

JAYCOR | 1 copy
11011 Forreyane Road
Post Office Box 85154
San Diego, California 92138
Attn: E. Venaas
F. Felbar

KAMAN Sciences Corporation | 1 copy each
Post Office Box 7463
Colorado Springs, Colorado 80933
Attn: Library

Lawrence Livermore National Laboratory | 1 copy each
University of California
Post Office Box 808
Livermore, California 94550
Attn: DOC CDN for 94550
DOC DCN for L-47 L. Wouters
DOC CDN for Tech. Infor. Dept. Lib.

Lockheed Missiles and Space Company, Inc. | 1 copy each
Post Office Box 504
Sunnyvale, California 94086
Attn: S. Taimlty
J.D. Weisner

Lockheed Missiles and Space Company, Inc. | 1 copy
3251 Hanover Street
Palo Alto, California 94304
Attn: J. Perez

Maxwell Laboratory, Inc. | 1 copy ea.
9244 Balboa Avenue
San Diego, California 92123
Attn: A. Kolb
M. Montgomery
J. Shannon

McDonnell Douglas Corporation | 1 copy
5301 Bolsa Avenue
Huntington Beach, California 92647
Attn: S. Schneider

Mission Research Corporation | 1 copy each
Post Office Drawer 719
Santa Barbara, California 93102
Attn: C. Longmire
W. Hart

Mission Research Corporation-San Diego 5434 Ruffin Road San Diego, California 92123 Attn: Victor J. Van Lint	1 copy
Northrop Corporation Northrop Research & Technology Center 1 Research Park Palos Verdes Peninsula, California 90274	1 copy
Physics International Company 2700 Merced Street San Leandro, California 94577 Attn: M. Krishnan C. Gilman S. Wong	1 copy
R and D Associates Post Office Box 9695 Marina Del Rey, California 90291 Attn: Library	1 copy each
Sandia National Laboratories Post Office Box 5800 Albuquereque, New Mexico 87115 Attn: Doc Con For 3141 D. McDaniel P. VanDevender K. Matzen, Code 4247	1 copy each
Science Applications, Inc. Post Office Box 2351 La Jolla, California 92038 Attn: R. Beyster	1 copy
Spectra Technol, Inc., 2755 Northup Way Bellevue, Washington 98004 Attn: Alan Hoffman	1 copy
Spire Corporation Post Office Box D Bedford, Massachusetts 07130 Attn: R. Little	1 copy
S-CUBED Post Office Box 1620 La Jolla, California 92038 Attn: A. Wilson	1 copy

Director | 1 copy each
Strategic Defense Initiative Organization
Pentagon 20301-7100
Attn: DE Lt. Col Richard Gullickson/DEO
IST Dr. Dwight Duston

Texas Tech University | 1 copy
Post Office Box 5404
North College Station
Lubbock, Texas 79417
Attn: T. Simpson

TRW Defense and Space Systems Group | 1 copy
One Space Park
Redondo Beach, California 90278
Attn: Technical Information Center

Naval Research Laboratory
Plasma Radiation Branch
Washington, D.C. 20375
Code 4720 - 50 copies
4700 - 26 copies
2628 - 22 copies